工學碩士 學位論文

초소형 마이크로 스트립 대역통과 필터

An Extremely Miniaturized Microstrip
Bandpass Filter

指 導 敎 授 姜 仁 鎬

2006年 8月

韓國海洋大學校 大學院

電 波 工 學 科

徐 海 燕

工學碩士 學位論文

초소형 마이크로 스트립 대역통과 필터

An Extremely Miniaturized Microstrip
Bandpass Filter

指 導 敎 授 姜 仁 鎬

2006年 8月

韓國海洋大學校 大學院

電 波 工 學 科

徐 海 燕

本 論文을 徐海燕의 工學碩士 學位論文으로 認准함.

委 員 長　　金 基 萬　　(印)

委　　員　　沈 俊 煥　　(印)

委　　員　　姜 仁 鎬　　(印)

２００６년 ６월

韓國海洋大學校 大學院

電波工學科

Contents

Nomenclature

f_0	:	Center frequency
Z_0	:	Characteristic Impedance
Z_{oo}	:	Odd mode characteristic Impedance
Z_{oe}	:	Even mode characteristic Impedance
θ	:	Electrical length of the transmission line
K	:	Coupling coefficient
λ	:	Wavelength

List of Tables

List of Fig.s

Abstract

Miniaturized microwave bandpass filters are always in demand for systems requiring small size and light weight. This demand is much increased recently by rapidly expanding cellular communication systems.

In this thesis, a novel miniaturized UHF bandpass filter using diagonally end-shorted coupled lines and lumped capacitors is proposed. With this new method, the size of the bandpass filter can be reduced to just a few degrees without sacrificing the characteristics of the conventional filter at the operating frequency. In addition to it, this new filter also shows a wider upper stopband.

A two-stage bandpass filter using this method has been designed and fabricated at a midband frequency of 300 MHz with electrical length of 5.2°. Both theoretical and experimental performances are presented. The total physical size of the fabricated filter is only 17 mm, 95% reduced compared with the conventional one. The fabricated filter exhibits good filtering characteristics with a wider upper stopband. This extremely miniaturized band-pass filter holds promise for MMIC (Monolithic Microwave Integrated Circuits) technologies which can be applied to mobile communications and other applications.

CHAPTER 1 Introduction

Filters form an indispensable component group in many RF/microwave applications. Nowadays, emerging applications continue to challenge filters with ever more stringent requirements. High performance bandpass filters with miniaturized size, narrow bandwidth, wide stopband and low cost are required in modern wireless communication systems, especially in mobile and portable internet systems. Planar filter structures which can be fabricated using printed-circuit technologies would be preferred whenever they are available and are suitable because of smaller sizes and lighter weight. Recent advance in high-temperature superconducting (HTS) circuits and microwave monolithic integrated circuits (MMIC) has additionally stimulated the development of various planar filters, especially narrow-band bandpass filters which play an important role in modern communications systems [1], [2].

A traditional end-coupled microstrip half-wavelength resonator filter is a typical narrow-band bandpass filter. In spite of that, at lower mobile communications bands, its physical length is too long, even on a higher dielectric constant substrate. Another disadvantage is that it has a spurious passband at $2f_{0,}$ where f_0 is the midband frequency of the filter. The $\lambda/2$ hairpin resonator [3] and slow-wave resonator filters [4] of planar structure are not only compact size due to the slow-wave effect, but also have a wider upper stopband resulting from the dispersion effect. However, this type of filters is still too large to be inserted into commercial transceiver system. The quarter wavelength ceramic combline filter having high dielectric material

[5] is another type of miniaturized bandpass filter. Nevertheless, the electrical length of the transmission line itself in this combline filter is not reduced. The lumped-element approach [6], [7], which uses spiral inductors and lumped capacitors leads to small circuit size, and this type of filter ideally does not have any spurious passband at all. However, the design of lumped-element circuits must be somewhat empirical, and it needs precise inductor models based on careful measurements of test elements. Moreover, the design becomes difficult at frequencies above 20 GHz.

In this thesis, a novel extremely miniaturized filter resulting from Hirota's reduced λ/4 transmission line is introduced. The size-reduction method proposing by Hirota [8] is attractive in view of using short transmission line and lumped capacitors. Nevertheless, the circuit size could not be much reduced due to the limitation of the high impedance of the transmission line. In this thesis, a new size-reduction method for λ/4 transmission line using diagonally end-shorted coupled lines and lumped capacitors is proposed. With this method, the size of the bandpass filter can be controlled arbitrarily in theory and reduced to just a few degrees without sacrificing the characteristics of the conventional filter at the operating frequency. In addition to it, this new filter shows a wider upper stopband. A two-stage bandpass filter is designed and fabricated at 300MHz to maximize the effect of size reduction method since the lower the resonant frequency, the longer the electrical length.

The contents of the thesis are illustrated as follows:

Chapter 1 briefly introduces the outline of this thesis, the background and the purpose of this work.

Chapter 2 presents a comprehensive circuit theory of size reduction method. This new method utilizes combinations of diagonally end-shorted coupled lines and shunt lumped capacitors. This chapter also explains the key factors which effect on the bandwidth of the filter.

Chapter 3 describes a design of two-stage bandpass filter in detail, including theoretical analysis, circuit design and simulated results by ADS and HFSS. The experimental results of the fabricated filter are also demonstrated and discussed.

Chapter 4 is the conclusion of this thesis. It summarizes the research work and proposes applications of this new type of filters.

CHAPTER 2 The theory of size reduction method

2.1 Introduction of filters

A microwave filter is a two-port network used to control the frequency response at a certain point in a microwave system by providing transmission at frequencies within the passband of the filter and attenuation in the stopband of the filter. There are general four types of filters: low-pass, high-pass, bandpass and bandstop. The low-pass filter allows low-frequency signals to be transmitted from the input to the output port with little attenuation. However, as the frequency exceeds a certain cut-off point, the attenuation increases significantly with the result of delivering an amplitude-reduced signal to the output port. The opposite behavior is true for a high-pass filter, where the low-frequency signal components are highly attenuated or reduced in amplitude, while beyond a cut-off frequency point the signal passes the filter with little attenuation. Bandpass and bandstop filters restrict the passband between specific lower and upper frequency points where the attenuation is either low (bandpass) or high (bandstop) compared to the remaining frequency band.

Filters have become indispensable devices not only in the field of telecommunication, but also in many other types of electrical equipment. Due to the variety and diversity of the filter types, it often becomes necessary for a designer to carefully consider which filter to adopt for a particular application.

2.2 Size reduction method

Miniaturized microwave bandpass filters are always in demand for systems requiring small size and light weight. This demand is much increased recently by rapidly expanding cellular communication systems. Although parallel–coupled microstrip filters with half-wavelength resonators are common elements in many microwave systems, their large size is incongruous with the systems where the size reduction is an important factor.

Planar filter structures which can be fabricated using printed-circuit technologies would be preferred whenever they are available and are suitable because of smaller sizes and lighter weight. The λ/2 hairpin resonator and slow-wave resonator filters of planar structure are not only compact size, but also have a wider upper stopband. However, this type of filters is still too large to be inserted into commercial transceiver system. Although the lumped-element approach, which uses spiral inductors and lumped capacitors, leads to small circuit size, they suffer from higher loss and poorer power handling capability.

The size-reduction method proposing by Hirota is attractive in view of using short transmission line and lumped capacitors. However, the circuit size could not be much reduced due to the limitation of the high impedance of the transmission line. It is therefore desirable to develop new types of microstrip bandpass filters which actually meet the requirement of small size.

2.2.1 Hirota's size reduction method for λ/4 transmission line

The reduced λ/4 transmission line using combinations of shortened transmission line and shunt lumped capacitors proposed by Hirota is shown in Fig. 1. A transmission line shorter than a quarter of a wavelength has a lower inductance and capacitance. The approach is to offset the inductance drop by increasing the characteristic impedance of the transmission line and to offset the capacitance loss by adding lumped capacitors. The **ABCD**-matrices of the circuits in Fig. 2.1 (a) and (b) are as follows,

$$[\mathbf{ABCD}] = \begin{bmatrix} 0 & jZ_0 \\ \dfrac{j}{Z_0} & 0 \end{bmatrix} \tag{2.1}$$

$$\begin{aligned} [\mathbf{ABCD}] &= \begin{bmatrix} 1 & 0 \\ j\omega C_1 & 1 \end{bmatrix} \begin{bmatrix} \cos\theta & jZ\sin\theta \\ j\dfrac{\sin\theta}{Z} & \cos\theta \end{bmatrix} \begin{bmatrix} 1 & 0 \\ j\omega C_1 & 1 \end{bmatrix} \\ &= \begin{bmatrix} \cos\theta - \omega C_1 Z\sin\theta & jZ\sin\theta \\ j\dfrac{\sin\theta}{Z} + 2j\omega C_1\cos\theta - j(\omega C_1)^2 Z\sin\theta & \cos\theta - \omega C_1 Z\sin\theta \end{bmatrix} \end{aligned} \tag{2.2}$$

where Z_0, Z, θ and ω are the characteristic impedance of the quarter-wavelength line, the characteristic impedance of the shortened line, the electrical length of the shortened line, and the

angular frequency, respectively.

(a)

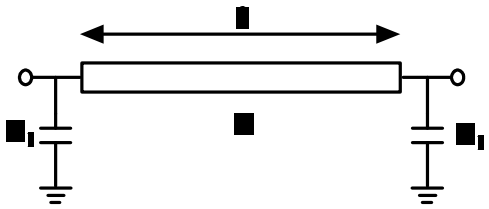

(b)

Fig. 2.1 λ/4 transmission line and its equivalent circuit. (a) λ/4 transmission line. (b) Shortened transmission line equivalent to the λ/4 transmission line.

From equation (2.1) and (2.2), we obtain

$$Z = Z_0/\sin\theta \tag{2.3}$$

$$\omega C_1 = (1/Z_0)\cos\theta \tag{2.4}$$

The characteristic impedance Z of the shortened line is inclined to be higher as the electrical length θ of the shortened line goes smaller.

If θ is very small, Z will become too high to attain. Up to now, the limitation of the electrical length of the transmission line is about π/8~π/12. Therefore, it is necessary to overcome the high impedance of the shortened transmission line.

2.2.2 New size reduction method

Fig. 2.2 (a) and (b) show the diagonally shorted coupled lines and its equivalent circuit [9]. The **ABCD**-matrix of the circuits is,

$$[\mathbf{ABCD}] = \begin{bmatrix} 1 & 0 \\ \dfrac{1}{jZ_{oe}\tan\theta} & 1 \end{bmatrix} \begin{bmatrix} \cos\theta & jZ\sin\theta \\ j\dfrac{\sin\theta}{Z} & \cos\theta \end{bmatrix} \begin{bmatrix} 1 & 0 \\ \dfrac{1}{jZ_{oe}\tan\theta} & 1 \end{bmatrix} \qquad (2.5)$$

The characteristic impedance of the diagonally shorted coupled lines is given by

$$Z = \frac{2Z_{oe}Z_{oo}}{Z_{oe} - Z_{oo}} \qquad (2.6)$$

We can see from the equation that the shorted coupled lines are proper for extremely miniaturized λ/4 transmission line since the high characteristic impedance can be easily attained by choosing $Z_{oe} \approx Z_{oo}$.

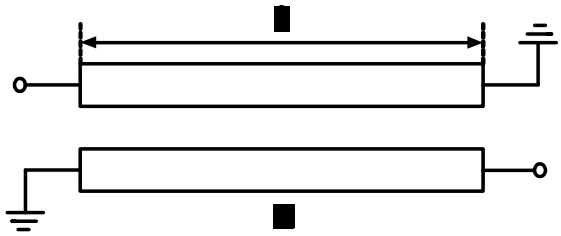

(a)

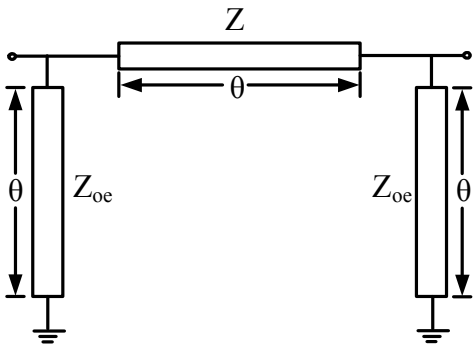

(b)

Fig. 2.2 (a) Diagonally shorted coupled lines. (b) Equivalent circuit of the coupled lines.

In Fig. 2.3 (a), the artificial resonance circuits are inserted to Hirota's lumped distributed λ/4 transmission line. The high impedance transmission line with shunt lumped inductors can be replaced by coupled lines shown in Fig. 3 (b). The parts in two dotted square boxes are equivalent when the following equations are satisfied [10]:

$$\omega L_0 = Z_{oe}\tan\theta \qquad (2.7)$$

$$\omega L_0 = \frac{1}{\omega C_0} \tag{2.8}$$

$$C = C_0 + C_1 \tag{2.9}$$

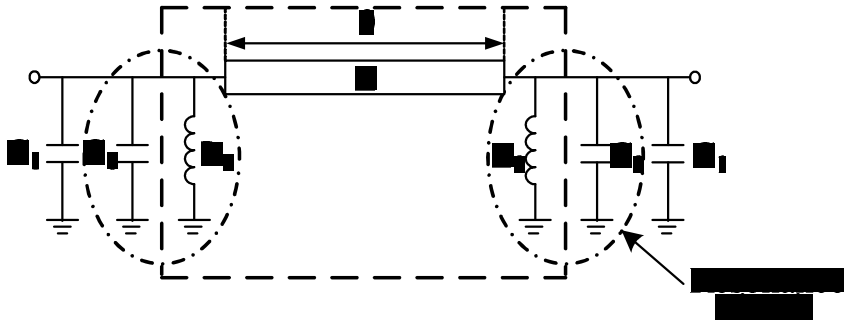

(a)

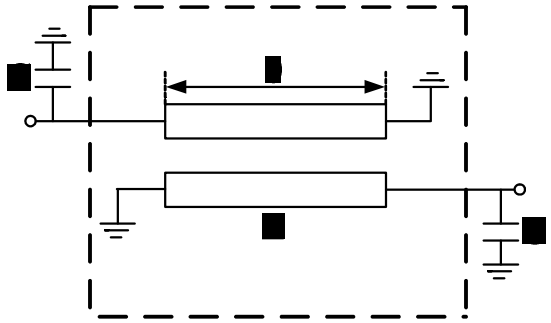

(b)

Fig. 2.3 (a) Equivalent circuit of Hirota's reduced-size λ/4 line including artificial resonance circuits. (b) The final equivalent λ/4 transmission line circuit.

The final miniaturized λ/4 transmission line is shown in Fig. 3 (b). It is feasible to obtain very high impedance using coupled lines. The peculiar feature of this extremely miniaturized λ/4 transmission line is that resonance circuits are located at edge sides of the transmission line. When the miniaturized λ/4 transmission lines are connected in series, the cascade circuit becomes a typical bandpass filter shown in Fig. 2.4, since the λ/4 section can be used as an admittance inverter.

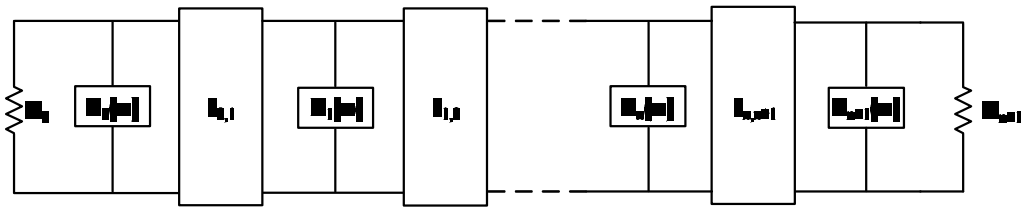

$B_n(\omega)$: Resonance circuit
$J_{n,n+1}$: Admittance inverter

Fig. 2.4 Generalized bandpass filter structure.

2.3 Bandwidth of the bandpass filter

However, due to the artificial resonance, the miniaturized filter has narrow bandwidth which can be controlled by the coupling coefficient since the bandwidth of diagonally end-shorted coupled line is closely related to the coupling coefficient [11]. In addition, another factor, the electrical length of the transmission line, may also affect the bandwidth of the filter. So it is necessary to investigate the relationship between the bandwidth, coupling coefficient and the electrical length of the circuit.

2.3.1 The coupling coefficient and the bandwidth.

In order to examine the relationship between the bandwidth and the coupling coefficient of the coupled lines, we first consider the phase variation of λ/4 transmission line.

In Fig. 2.5, Y_{11} and Y_{22} are respectively the driving–point admittance at port 1 and port 2. Y_{12} and Y_{21} are respectively the reverse transfer admittance and the forward transfer admittance.

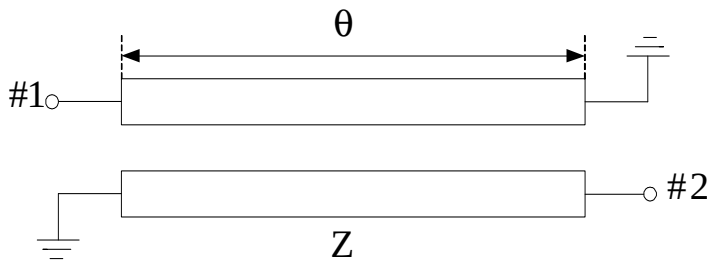

Fig. 2.5 The shorted coupled lines.

The admittance matrix is as follows,

$$[\mathbf{Y}] = \begin{bmatrix} Y_{11} & Y_{12} \\ Y_{21} & Y_{22} \end{bmatrix} = \begin{bmatrix} -j\dfrac{Y_{oo}+Y_{oe}}{2}\cot\theta & -j\dfrac{Y_{oo}-Y_{oe}}{2}\csc\theta \\ -j\dfrac{Y_{oo}-Y_{oe}}{2}\csc\theta & -j\dfrac{Y_{oo}+Y_{oe}}{2}\cot\theta \end{bmatrix} \tag{2.10}$$

Since the circuit is symmetric, $Y_{11}=Y_{22}$ and $Y_{12}=Y_{21}$ are obtained.

The characteristic admittance of the coupled lines is,

$$Y = \frac{Y_{oo} - Y_{oe}}{2} \tag{2.11}$$

Fig. 2.6 shows an equivalent circuit of the shorted coupled lines.

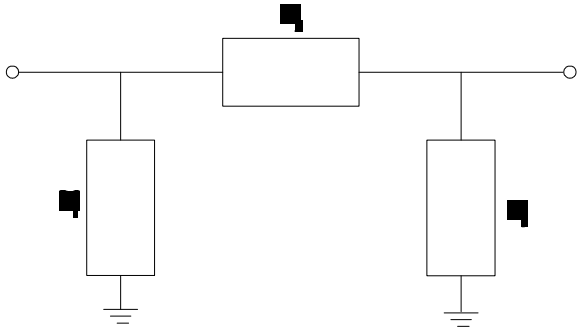

Fig. 2.6 The equivalent circuit of the shorted coupled lines.

The admittance parameters are expressed as follows:

$$Y_1 = Y_{11} + Y_{12} = -j\frac{Y_{oo} + Y_{oe}}{2}\cot\theta + j\frac{Y_{oo} - Y_{oe}}{2}\csc\theta = Y_3 \tag{2.12}$$

$$Y_2 = -Y_{12} = j\frac{Y_{oo} - Y_{oe}}{2}\csc\theta \tag{2.13}$$

If capacitors are added to each side of the circuit shown in Fig. 2.7, it becomes the equivalent circuit of the miniaturized λ/4 transmission line in Fig. 2.3 (b).

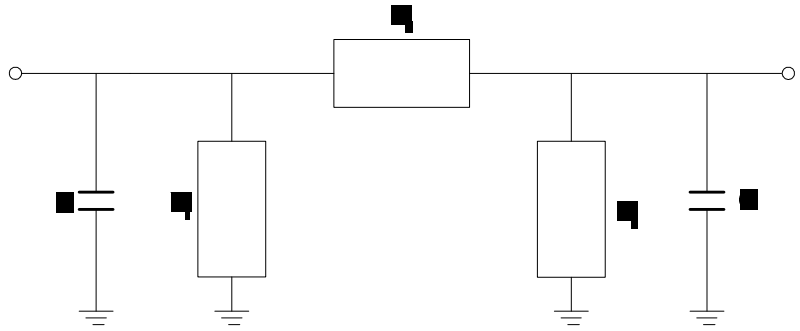

Fig. 2.7 An equivalent circuit of the miniaturized λ/4 transmission line.

The Y-parameters of the circuit in Fig. 2.7 are as follows,

$$Y'_{11} = Y_{11} + j\omega C \tag{2.14}$$

$$Y'_{12} = -Y_{12} \tag{2.15}$$

The admittance matrix is,

$$\left[\mathbf{Y}'\right] = \begin{bmatrix} Y_{11}' & Y_{12}' \\ Y_{21}' & Y_{22}' \end{bmatrix} = \begin{bmatrix} -j\frac{Y_{oo}+Y_{oe}}{2}\cot\theta + j\omega C & j\frac{Y_{oo}-Y_{oe}}{2}\csc\theta \\ j\frac{Y_{oo}-Y_{oe}}{2}\csc\theta & -j\frac{Y_{oo}+Y_{oe}}{2}\cot\theta + j\omega C \end{bmatrix} \tag{2.16}$$

S_{21} of the circuit in Fig. 2.3 (b) can be represented as follows,

$$S_{21} = \frac{-2Y_{21}'Y_0'}{\Delta Y'} \times (-1) \tag{2.17}$$

$$Y_0' = Y_0 = \frac{1}{Z_0} \tag{2.18}$$

$$\Delta Y' = (Y_{11}' + Y_0')(Y_{22}' + Y_0') - Y_{12}'Y_{21}' \tag{2.19}$$

Upon using equation (2.18) and (2.19), S_{21} is obtained,

$$S_{21} = \frac{j(Y_{oo} - Y_{oe})\csc\theta \times Y_0}{\left(Y_0 - j\frac{Y_{oo}+Y_{oe}}{2}\cot\theta + j\omega C + j\frac{Y_{oo}-Y_{oe}}{2}\csc\theta\right) \times \left(Y_0 - j\frac{Y_{oo}+Y_{oe}}{2}\cot\theta + j\omega C - j\frac{Y_{oo}-Y_{oe}}{2}\csc\theta\right)} \tag{2.20}$$

Thus, the phase of S_{21} in the miniaturized $\lambda/4$ transmission line can be represented as follows:

$$\frac{3}{2}\pi + \tan^{-1}\frac{1}{Y_0}\left[\frac{Y_{oo}+Y_{oe}}{2}\cot\theta - \omega C - \frac{Y_{oo}-Y_{oe}}{2}\csc\theta\right] + \tan^{-1}\frac{1}{Y_0}\left[\frac{Y_{oo}+Y_{oe}}{2}\cot\theta - \omega C + \frac{Y_{oo}-Y_{oe}}{2}\csc\theta\right] \tag{2.21}$$

Since the coupling coefficient

$$K = \frac{Y_{oo} - Y_{oe}}{Y_{oo} + Y_{oe}} \tag{2.22}$$

From equation (2.11) and (2.22), we obtain,

$$\frac{Y_{oo} + Y_{oe}}{2} = \frac{Y}{K} \tag{2.23}$$

Then the phase of S_{21} can be adjusted as follows,

$$\frac{3}{2}\pi + \tan^{-1}\frac{1}{Y_0}\left[\frac{Y}{K}\cot\theta - \omega C + \frac{Y}{\sin\theta}\right] + \tan^{-1}\frac{1}{Y_0}\left[\frac{Y}{K}\cot\theta - \omega C - \frac{Y}{\sin\theta}\right] \tag{2.24}$$

From the equation (2.24) we can see that the phase of S_{21} is fixed to $3\pi/2$ regardless of all the value of k if θ equals 90°. However, as θ changes from 90°, the phase will deviate from $3\pi/2$. In order to minimize this phase variation, the value of k should be increased. Hence, the result is obtained that the bandwidth increases as the coupling coefficient increases. Fig. 2.8 (a) and (b) simulated using Agilent ADS illustrate the relation between the bandwidth and the coupling coefficient of the filter. The designed parameters of the filtes are shown in Table 2.1.

Table 2.1 Parameters of filters for different coupling coefficients.

[redacted]	[redacted]	
[redacted]	[redacted]	[redacted]
	[redacted]	[redacted]
	[redacted]	[redacted]
[redacted]	[redacted]	[redacted]
	[redacted]	[redacted]
	[redacted]	[redacted]
[redacted]	[redacted]	[redacted]
	[redacted]	[redacted]
	[redacted]	[redacted]

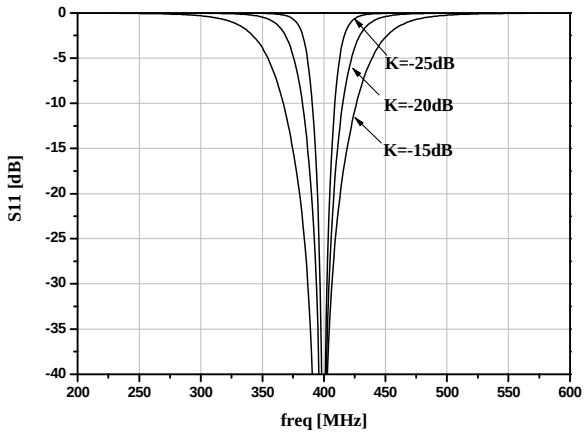

(a)

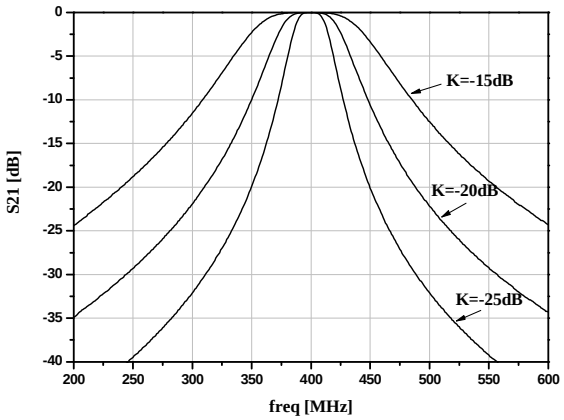

(b)

Fig. 2.8 Relation between the coupling coefficient and the bandwidth of the filter. (a) $S_{11.}$ (b) $S_{21.}$

2.3.2 The electrical length and the bandwidth.

As the relation between the electrical length and the bandwidth of the filter is difficult to be figured out from the equation (2.24), we use ADS to simulate the circuits in different electrical lengths shown in Fig. 2.9. Table 2.2 shows the designed parameters of filters.

Table 2.2 Parameters of filters for different electrical length.

[redacted]	[redacted]	
[redacted]	[redacted]	[redacted]
	[redacted]	[redacted]
	[redacted]	[redacted]
[redacted]	[redacted]	[redacted]
	[redacted]	[redacted]
	[redacted]	[redacted]
[redacted]	[redacted]	[redacted]
	[redacted]	[redacted]
	[redacted]	[redacted]

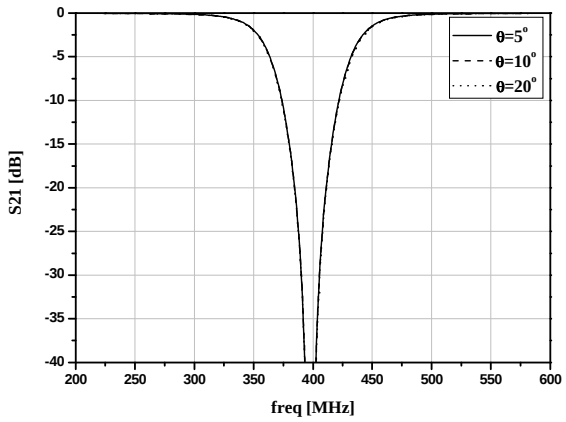

(a)

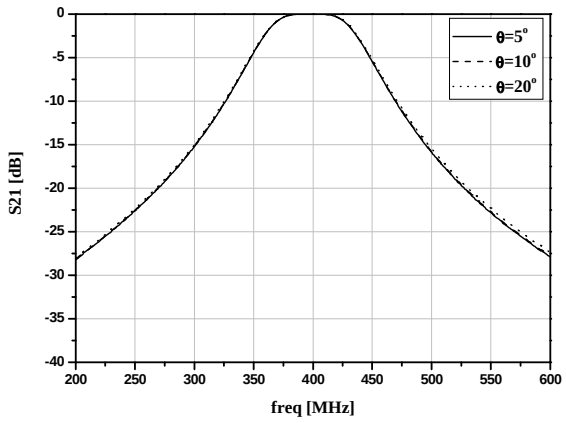

(b)

Fig. 2.9 Relation between the bandwidth of the filter and the electrical length of the coupled lines. (a) $S_{11.}$ (b) $S_{21.}$

As shown above, the bandwidth of the filter nearly keeps same as the electrical length changes. Thus, the main factor to affects the bandwidth of the filter is the coupling coefficient, while the electrical length has just little effect on the bandwidth.

CHAPTER 3 **Simulation and experiment results**

3.1 A design of a 300 MHz bandpass filter

In this paper, an extremely miniaturized band-pass filter for f_0=300MHz, Z_0=50Ω is designed. The electrical length of the coupled lines is 5.2 degree. The one-stage and two-stage bandpass filters and their simulation results in ADS are shown in Fig. 3.1 and Fig. 3.2.

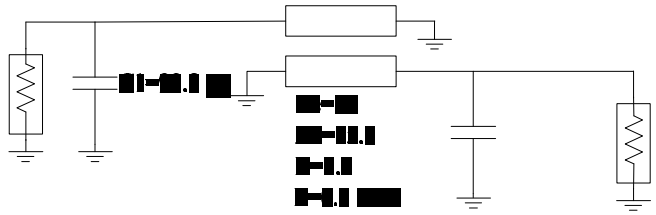

(a)

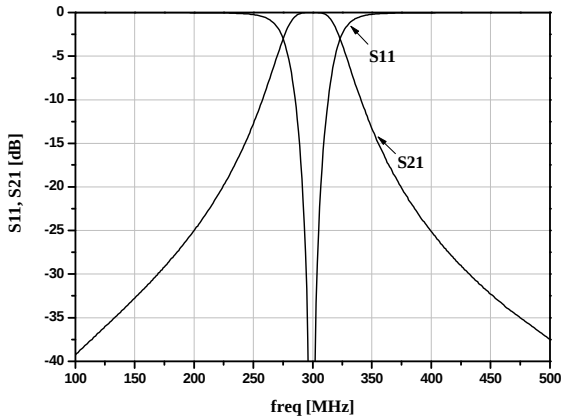

(b)

Fig. 3.1 One-stage bandpass filter. (a) Circuit. (b) Simulation result.

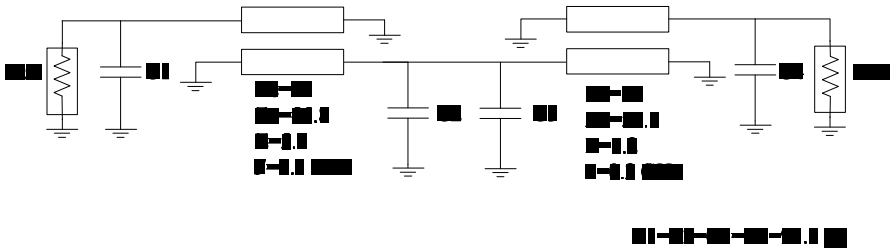

(a)

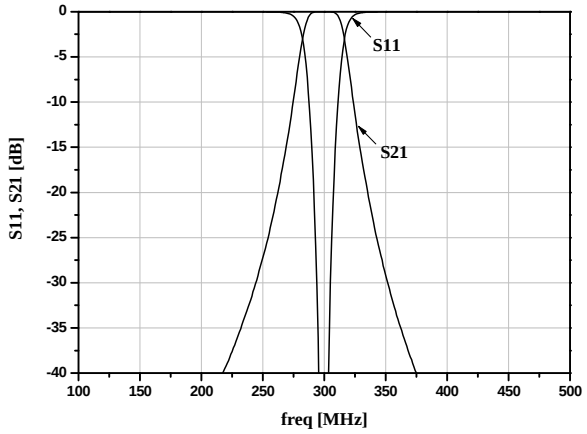

(b)

Fig. 3.2 Two-stage bandpass filter. (a) Circuit. (b) Simulation results.

3.2 The effect of the inter-stage part

For the actual circuit, the inter-stage part is very important because there is some coupling between two resonators. Fig. 3.3 shows an extremely miniaturized two-stage bandpass filter with a small transmission line in the middle which connects two resonators. In order to investigate the inter-stage line length effecting on the characteristics of the filter, a group of two-stage bandpass filters with different inter-stage line length are simulated in HFSS.

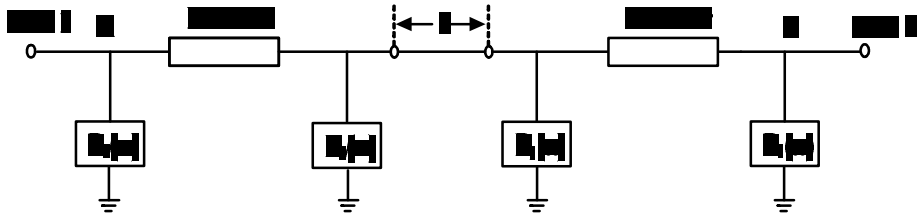

Fig. 3.3 An extremely miniaturized two-stage bandpass filter.

Fig. 3.4 (a) and (b) show the layouts of the two-stage bandpass filter drawing in HFSS, and their corresponding simulation results are illustrated in Fig. 3.5 (a) and (b). We can see from the Fig. 3.5 that the inter-stage transmission line is indispensable and the filtering characteristics get better as the line length is longer.

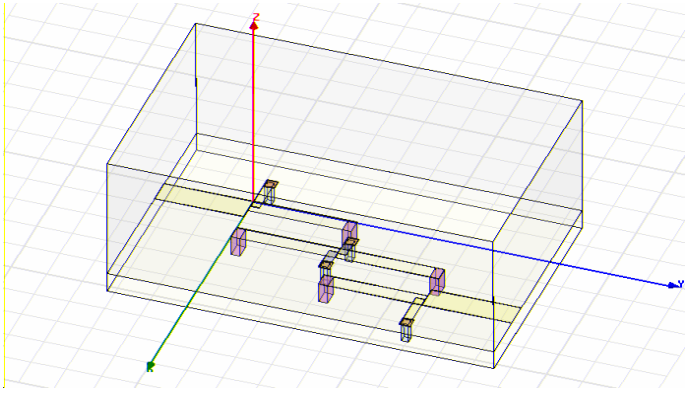

(a)

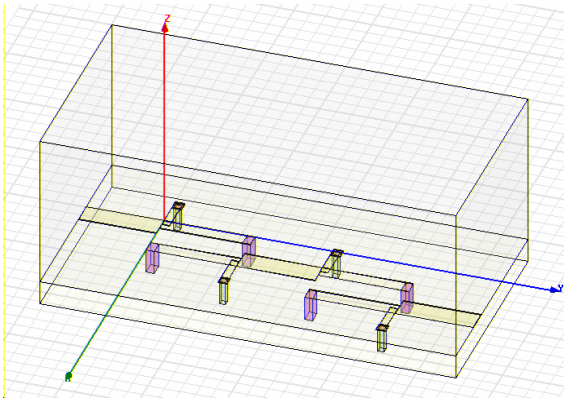

(b)

Fig. 3.4 Layouts of the bandpass filter in HFSS. (a) Two-stage filter without inter-stage line. (b) Two-stage filter with a small inter-stage transmission line.

When two miniaturized λ/4 transmission lines are connected directly shown in Fig. 3.4 (a), a distorted shape appears in Fig. 3.5. This is resulted from an unwanted coupling which can not be neglected. The key factor which gives rise to the coupling effect is that the phase difference between edge sides of cascade two stages is 180° and the distance between two points is too close. Therefore, it is

necessary to insert a very short transmission line to block the unwanted coupling between two resonators.

When the bandpass filters with the small inter-stage transmission line, for example the line length L=3 mm and L=5 mm (Fig. 3.4 (b)), are simulated by HFSS, the filter operates normally as shown in Fig. 3.5.

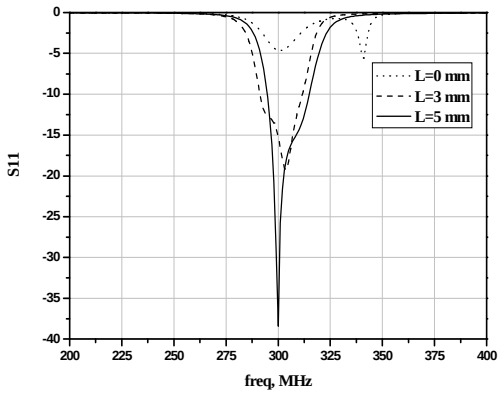

(a)

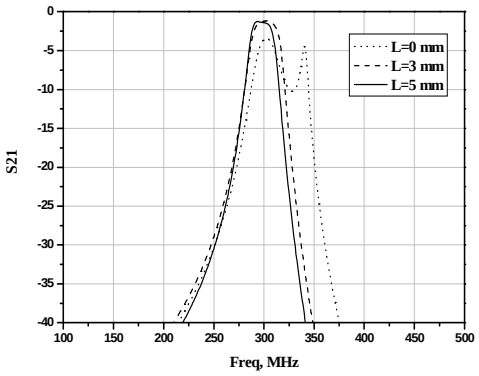

(b)

Fig. 3.5 (a) S_{11} for different lengths of the inter-stage line. (b) S_{21} for

different lengths of the inter-stage line.

To our knowledge, this small inter-stage transmission line between resonators has not been reported in literature before. However, as the size of the filter becomes smaller, the small transmission line is needed. Considering the size of the circuit, 5mm is chosen for our design as the length of the inter-stage line.

3.3 Fabrication and measurement

The extremely miniaturized band-pass filter is fabricated on a 1.57mm-thick Teflon substrate with a relative permittivity of 10 and a conductor thickness of 35um. Fig. 3.6 shows the layout of the filter.

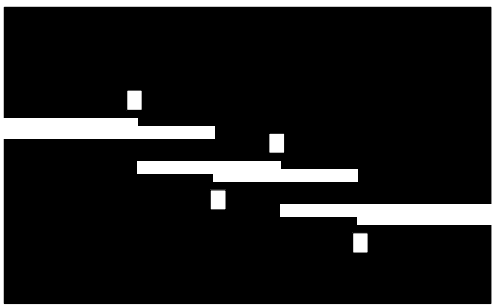

Fig. 3.6 Layout of the designed bandpass filter.

The physical dimensions of transmission lines for the filter are illustrated in Table 3.1.

Table 3.1 Physical dimensions of transmission lines for the filter.

Coupled lines (50Ω)	W	0.9 mm
	S	1.7 mm
	L	5.8 mm
Inter-stage line (50Ω)	W	1.5 mm
	L	5 mm
Port lines (50Ω)	W	1.5 mm
	L	10 mm
Total length	L_T	17mm

A photograph of the fabricated filter with the total physical length 1.7 cm is shown in Fig. 3.7.

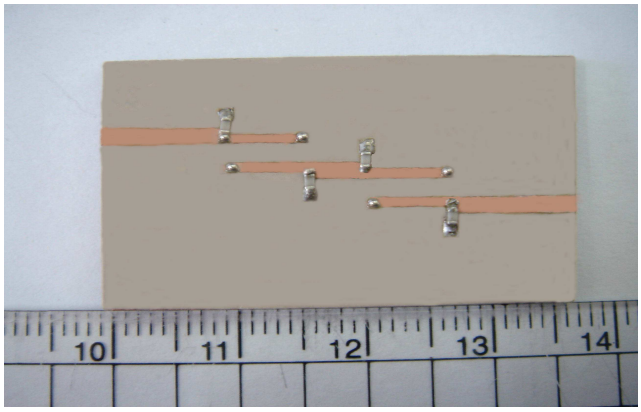

Fig. 3.7 Photograph of the fabricated bandpass filter.

The MIM (Metal Insulator Metal) capacitors are used for simulation because the structure of the actual capacitor- Chip monolithic Ceramic Capacitor，is too complex to simulate in HFSS. Fig. 3.8 shows the structure of MIM capacitors for the filter simulation.

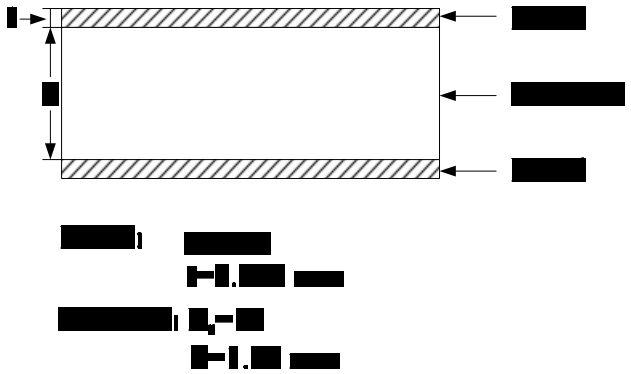

Fig. 3.8 Structure of the MIM capacitor used for simulation in HFSS.

Fig. 3.9 (a) and (b) illustrate the comparison of the HFSS simulation and experimental results. We can see from the figure that the measured S-parameters agree well with the simulated ones. In Fig. 3.9 (a), the measured S_{11} is -30 dB at the operating frequency 302 MHz. The insertion loss is -4.3 dB at the operating frequency shown in Fig. 3.9 (b). The measured results of the experimental filter are summarized in Table 3.2.

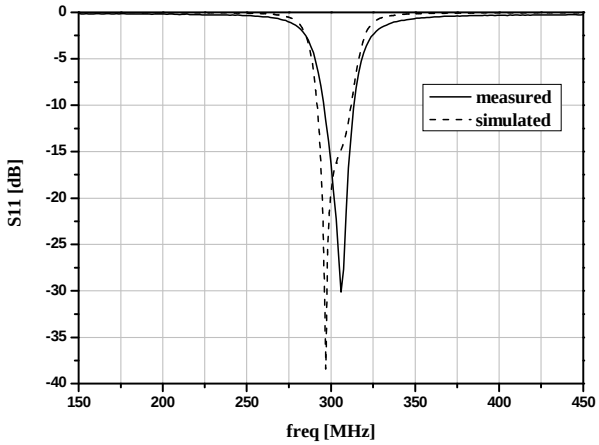

(a)

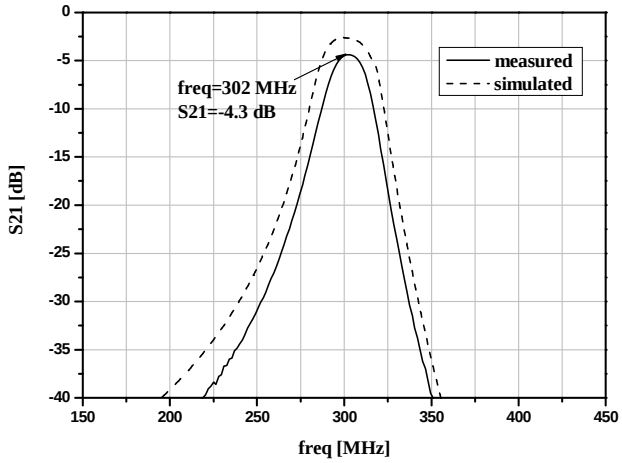

(b)

Fig. 3.9 Simulated and measured results. (a) $S_{11.}$ (b) S_{21}.

Table 3.2 Measured results of the experimental filter.

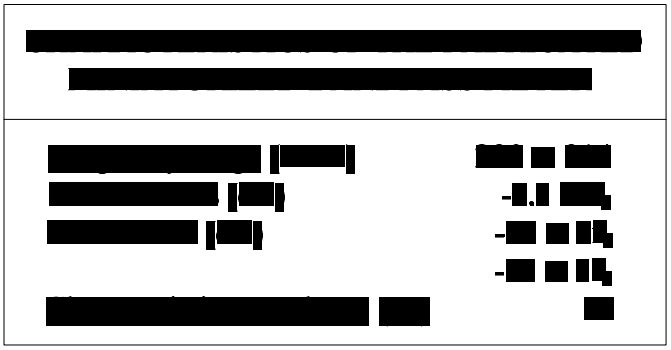

3.4 The harmonic suppression

In many filter applications, in order to reduce interference by keeping out-of-band signals from reaching a sensitive receiver, a wider upper stopband is required. However, many planar bandpass filters which are comprised of half-wavelength resonators have inherently a spurious passband at $2f_{0,}$ where f_0 is the midband frequency. A cascade lowpass or bandstop filter may be used to suppress the spurious passband at the cost of extra insertion loss and size. Lumped element filters ideally do not have any spurious passband at all, but they suffer from higher loss and poorer power handling capability. Bandpass filters using stepped impedance resonators (SIR) [12] or end-coupled slow-wave resonators [13] are able to control spurious response, but they can only be implemented in fewer filtering configurations.

The slow-wave open-loop resonator filters proposed by J. Hong

can also suppress harmonics. This type of filters includes a series of capacitively loaded transmission line resonators. When the loading capacitance is increased, the resonant frequencies are shifted down, while the ratio of the first spurious resonant frequency to the fundamental one is increased which would attributes to the increase of the dispersion. Thus, a wide upper stopband is obtained by shifting the spurious frequencies from the integer multiple of the fundamental frequency. However, as the first spurious frequency can only be shifted to the position which is a few times of the fundamental frequency, it is difficult for the slow-wave open-loop resonator filters to get a very wide upper stopband.

In this thesis, the proposed filter is reduced to just a few degrees using combinations of diagonally end-shorted coupled lines and shunt lumped capacitors. Therefore, the first spurious frequency can be shifted to very high frequency for the electrical length of the resonant is very small. In our case, the first spurious frequency is shifted to the position which is more than 30 times of the fundamental frequency as the electrical length of the designed coupled-line resonators are only 5.2°. No spurious response occurs for the frequency below 10 GHz.

As shown in Fig. 3.10, the broadband transmission characteristics of the fabricated filter. It illustrate that the filter has a tremendously wider upper stopband below -45 dB up to 7 f_0.

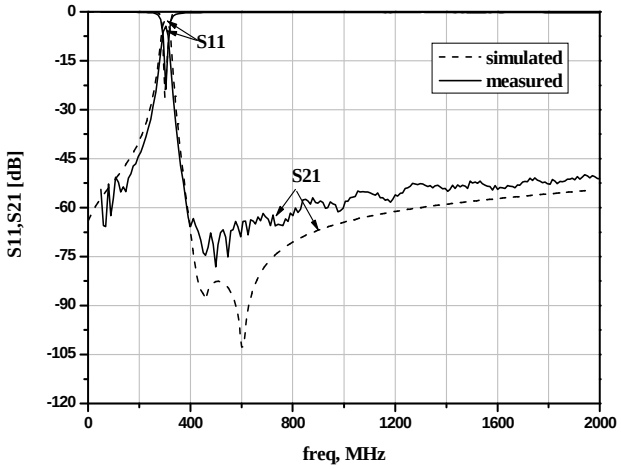

Fig. 3.10 Simulated and measured S-parameter of filter in broad range.

CHAPTER 4 **Conclusion**

In this thesis, we have presented both the theory and experiment of an extremely miniaturized band-pass filter using combination of diagonally end-shorted coupled lines and lumped capacitors. Using this new reduction method, the size of the bandpass filter can be controlled arbitrarily in theory and reduced to just a few degrees without sacrificing the characteristics of the conventional filter at the operating frequency. In addition to it, this type of filters has a wider upper stopband. Through analysis, we also obtain that the bandwidth of the filter is mostly influenced by the coupling coefficient, and the bandwidth increases as the coupling coefficient increases.

A two-stage bandpass filter is designed and fabricated at a midband frequency of 300MHz. The measured results agree well with the theoretical ones. The fabricated bandpass filter is reduced by more than 95% compared with the conventional one and has a wider upper stopband with the first spurious response at the frequency up to 10 GHz. It can be seen that this extremely miniaturized band-pass filter holds promise for MMIC (Monolithic Microwave Integrated Circuits) technologies applied to mobile communications and other applications.

References

[1] A. F. Sheta, K. Hettak, J. Ph. Coupez, C. Person, S. Toutain, and J. P. Blot, " A new semi-lumped microwave filter structure," *IEEE MTT-S Dig.*, pp. 383-386, 1995.

[2] G. L. Matthaei, N. O. Fenzi, R. Forse, and S. Rohlfing, "Narrow-band hairpin-comb filters for HTS and other applications," *IEEE MTS-S Dig.*, pp. 457-460, 1996.

[3] M. Sagawa, K. Takahashi, and M. Kakimoto, "Miniaturized hairpin resonator filters and their application to receiver front-end MICs," *IEEE Trans. Microwave Theory Tech.*, vol. 37, pp. 1991-1997, 1989.

[4] J. Hong and M. J. Lancaster, "Theory and experiment of novel microstrip slow-wave open- loop resonator filters,", *IEEE Trans. Microwave Theory Tech.*, vol. 45, pp. 2358-2365, 1997.

[5] H. Yao, C Wang, and K. Zaki, "Quarter wavelength ceramic combline filter," *IEEE Trans. Microwave Theory Tech.*, vol. 44, no. 12, pp. 2673-2679, 1996.

[6] M. Caulton, B. Hershenov, S. P. Knight, and R. E. Debrecht, "Status of lumped elements in microwave integrated circuits-Present and future," *IEEE Trans. Microwave Theory Tech.*, vol. MTT-19, pp. 588-599, July 1971.

[7] J. Putnam, and R. Puente, "A monolithic image-rejection mixer on GaAs using lumped elements," *Microwave J.*, vol. 30, no. 11, pp. 107-116, Nov. 1987.

[8] T. Hirota, A. Minakawa and M. Muraguchi, "Reduced-size Branch-line and Rat-Race Hybrids for Uniplanar MMIC's," *IEEE*

Trans. Microwave Theory Tech., vol. 38, no. 3, pp. 270-275, 1990.

[9] G. Matthaei, L. Young, E. M. T. Jones, Microwave Filters, Impedance-Matching networks, and Coupling Structures, Artech House, pp.220.

[10] I. Kang and J. Choi, “A New reduced-size lumped distributed power divider using the shorted coupled line pair”, *Korea Electromagnetic Engineering Conference*, vol.13, No.1, pp283-287, Nov. 2003.

[11] I. Kang and K. Wang, “A broadband rat-race ring coupler with tight coupled lines,” *IEICE Communications*, vol.e88-B, no.10, pp. 4087-4089, 2005.

[12] M. Makimoto and S. Yamashita, “Bandpass filters using parallel coupled stripline stepped impedance resonators,” *IEEE Trans. Microwave Theory Tec*h., vol. MTT-28, pp. 1413-1417, 1980.

[13] J. S. Hong and M. J. Lancaster, “End-coupled microstrip slow-wave resonator filter,” *Electron. Lett.*, vol. 32, pp.1494-1496, 1996.

Acknowledgement

I would like to express my heartfelt gratitude and respect to those who have helped me during the last two years. This thesis would not have been possible without the support and assistance that I received from them.

My sincere thanks are due to my advisor, Professor In-ho Kang. His wide knowledge, strict research attitude and enthusiasm in work deeply impressed me and taught me what a true scientific research should be. I am also thankful to the other Professors of our department for their supports and guidance on this work, who are Professor Dong Il Kim, Professor Kyeong-Sik Min, Professor Hyung Rae Cho, Professor Ki Man Kim, Professor Ji Won Jung, Professor Young Yun, Professor Joon hwan Shim and Professor Dong Kook Park in Department of Electronic and Communication Engineering. .

My gratitude also goes to our senior Mr. Rui Li for his timely and unselfish help. Certainly, I can not be thankful enough to our laboratory members Mr. Kai Wang and Mr. Shiwei Shan. They not only help me on my research work, but also let me enjoy the friendly work environment. My heartfelt thanks are also due to the friends in Microwave and Antenna lab, Mr. Tea kyoung Han, Mr. Yong Gun Seo and others who offered me great helps in my experiments.

I would like to acknowledge all my Chinese friends, especially my

roommate Shanshan Jiang who gives me supports and encouragement all the time.

Finally, I would like to express my sincere thanks to Professor Yingji Piao and Teacher Zheng Li from Qingdao University of China. Without their recommendation, it is impossible for me to get the opportunity to study in Korea.